COBEM 2023 27TH INTERNATIONAL CONGRESS OF MECHANICAL ENGENEERING

ABCM Brazilian Society of Mechanical Sciences and Engineering
27th ABCM International Congress of Mechanical Engineering
December 04-08, 2023, Florianópolis-SC, Brazil

COB-2023-1143
INVESTIGATION OF A MAGNETIC ANTI-SCALING DEVICE FOR FOULING MITIGATION IN VALVES

Daniel Imbelloni Costa e Silva Morais
Caroline de Oliveira Gonçalves
Luise da Silva Santos de Oliveira
Matheus Moraes de Jesus Paz
Matheus Moerbeck de Almeida Rego Murtha
Mateus Gonçalves Ferreira Rodrigues d'Almeida
Juliana B. R. Loureiro
Universidade Federal do Rio de Janeiro, NIDF - Núcleo Interdisciplinar de Dinâmica de Fluidos PEM/COPPE/UFRJ, CT2, Bloco2, C.P. 68503, Cep. 21.941-972, Rio de Janeiro, RJ, Brazil.
jbrloureiro@mecanica.coppe.ufrj.br
André Leibsohn Martins
PETROBRAS/CENPES - Cidade Universitária - Rio de Janeiro, RJ, Brazil
aleibsohn@petrobras.com.br

Abstract. *Fouling is a complex phenomenon that is influenced by several variables such as pressure, temperature, flow rate and salt concentration. Thus, this work aims to experimentally evaluate the action of the magnetic field to reduce scale inside pipes. Calcium chloride and sodium bicarbonate solutions were used as incompatible brines for the formation of the inorganic scale. The Sliding-Sleeve completion valve was used along the pipeline in different positions and in the 50% opening condition. The magnetic device used was the square magnet, which has 0.55 Tesla in the attractive configuration, and its influence was analyzed at different positions along the flow loop. Thus, this work had the specific objective of mitigating fouling by analyzing different valve and magnet positions in the Multipurpose Flow Simulator. The flow rates of the two injection lines were controlled, and absolute pressure measurements were taken along the pipeline and differential pressure in the smart valve, in addition to pH, conductivity and temperature measurements. After the experiment, the fouling masses deposited in different positions along the flow loop were analyzed. It was observed that the magnetic field had the effect of delaying the time for blocking the sliding sleeve valve, when positioned close to the valve, the best case being the valve positioned 28 m from the injection with the magnet positioned upstream of the valve and at a Reynolds number of 9,650.*

Keywords: *magnetic fields, scale, valves.*

1. INTRODUCTION

Calcium carbonate fouling is a complex phenomenon whose consequences can be very detrimental to the industry. The influence of physical methods on fouling control has been the focus of research since the 1970s. Although the literature report a significant decrease in deposition due to the effect of the magnetic field, the working principle is still poorly understood. Thus, this work aims to experimentally evaluate the performance of physical methods to mitigate fouling in pipes. Specifically, the present work analyses the influence of the magnetic field on the fouling formation in a pipe flow. The experimental conditions cover different positions of the Sliding-sleeve valve as well as the magnetic field, subjected to two different Reynolds numbers in the Multipurpose Flow Simulator.

2. LITERATURE REVIEW

Incrustation becomes a problem when it leads to the reduction, total or partial, of the flow conduits, providing a head loss greater than expected, which reduces the productivity of the system. Therefore, some terms commonly found in the literature refer to incrustation, alluding to other systems that can be blocked. Oddo and Tomson (1989) presented a brief collection of these terms: scale, fouling, sediment, sludge, gyp, incrustation, calculus, and stone. Kokal and Sayegh (1995), for example, call asphaltenes the "cholesterol" of petroleum.

The incrustation of inorganic substances in oil extraction pipes is directly related to the change in the physicochemical properties of the fluid when flowing out of the well, such as pressure, temperature and turbulence. Calcium carbonate, CaCO3, for example, has relatively low solubility in water; however, its solubility increases at high partial pressures of CO2. Thus, due to sudden changes in those physicochemical quantities, calcium carbonate tends to precipitate, forming incrustations.

Prior to the start of drilling and production, the dissolved species, precursors to fouling, are in steady state with the reservoir environment. Some authors call this an equilibrium state (Haghighi (2009)), but as a result of geothermal flows and the gravitational field, the fluid inside the reservoir is in a steady state of flow (Nikpoor *et al.* (2016); Obidi *et al.* (2017) . However, after drilling, precipitation reactions begin to occur when external forces act on the fluids, that is, when there is a disturbance that favors the imbalance after thousands of years of thermal, chemical and mechanical interaction between rock and fluids. These external forces are mainly due to runoff and its consequences, and to the mixing of fluids – mainly the mixing of reservoir water with other waters, such as injection water – incompatible in terms of chemical species. The flow of fluids will imply directly on several aspects, namely: i) on the shear rate, which influences the growth and agglomeration of particles (Liu and Dreybrod (1997); Nichols *et al.* (2016); Yan *et al.* (2017a,b)), ii) in their transport to regions at different temperatures, which may affect the solubility of some inorganic salts (Cowan and Weintritt (1976); Frenier and Ziauddin (2008)), iii) in pressure reduction, which affects the solubility of some inorganic salts (Cowan and Weintritt (1976)), iv) in addition to favoring the release of gases dissolved in the formation water, such as CO2 (Rousseau *et al.* (2001); Shepherd (2008)), an important component of the equilibrium reaction of calcium carbonate (Auerbach *et al.* (1983); Mackay *et al.* (2003)).

In reservoirs, precipitation is mainly due to the mixing of incompatible waters in terms of chemical species (Nasr-El-Din and Al-Humaidan (2001); Merdhah (2007)), which can favor the deposition of inorganic compounds, such as calcium sulfates (CaSO4) , barium (BaSO4), and strontium (SrSO4). This is the typical case in water injection campaigns (*waterflooding*), mainly when using sea water (Taheri *et al.* (2008)). When deposition occurs in the reservoirs, the result can be even more disastrous, mainly due to the inaccessibility for mitigation of the problem, which could lead to permanent damage to the formation (Szikszay (1993)).

3. METHODOLOGY

The experimets were conducted at the Multipurpose Flow Loop of the Laboratory of Well Technology in Engineering - LTEP, located in CT2 of the Federal University of Rio de Janeiro - UFRJ. It is worth noting that the structure used is part of the Interdisciplinary Center for Fluid Dynamics – NIDF, also located at CT2 at UFRJ.

The installed structure has sections of 304L steel and acrylic tubes, tanks for storing saline solutions and water, pumps, meters and other characterization equipment.

All the tests presented here were carried out in an open circuit, in order to simulate conditions closer to the real application. In these tests, both solutions are injected at the beginning of the pipeline, as shown in Figure 1. The flow rates of the two injection lines were controlled, and absolute pressure measurements were taken along the pipeline and differential pressure in the smart valve, in addition to pH, conductivity and temperature measurements.

To carry out the tests, two saline solutions were prepared: sodium bicarbonate NaHCO3 and calcium chloride dihydrate CaCl2. 2H2O. These solutions remained in the process of homogenization and stabilization for five days in a tank open to the atmosphere, subject to a mixer. The water used to prepare the solutions and the ready-made solutions were chemically characterized based on pH, conductivity and temperature measurements.

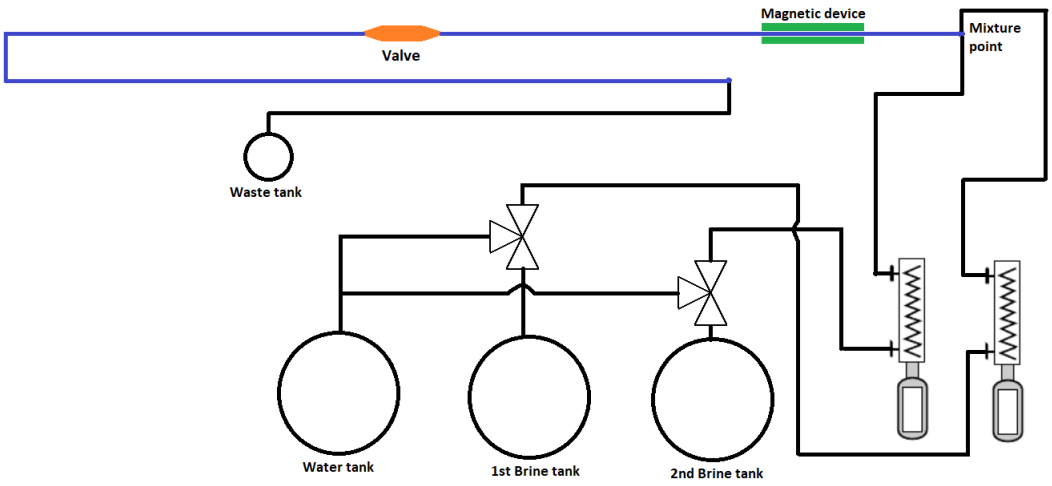

Figure 1. Schematic diagram of the Multipurpose Flow Loop with the magnetic field and the sliding-sleeve valve.

The characteristics of the flow loop used can be found in the Table 1.

In the experimental tests presented here, the conditions of the sodium bicarbonate and calcium chloride reservoirs are shown in Table 2.

The prototype of the Sliding-Sleeve completion valve was used in the 50% open condition (16 mm) in pipe length

Table 1. Flow loop features.

Test Section Material	Steel
Pipe length (m)	70
External diameter (mm)	15
Internal diameter (mm)	11
Valve mass (g)	183.7322

Table 2. Physico-chemical conditions of the saline solutions used in the scale tests.

	Concentration (g/L)	Molarity (mol/L)	Conductivity (mS/cm)	pH
NaHCO3	12.60	0.15	10.87	9.1-9.3
CaCl2	7.35	0.05	9.5	7.2-7.6

positions of 0.7 m, 3 m, 28 m, 41 m and 45.6 m from the injection and is represented in Figure 2.

Figure 2. Prototype of Slide Sleeve Completion Valve.

The magnetic device used was the so-called gray magnet as can be seen in Figure 3 which has 0.55 Tesla. This magnetic device was used in attractive as well as repulsive configuration at the following positions along the pipe length: 0.37 m from the injection downstream of the solution tanks or 0.38 m upstream of the valve. In Table 3 some important parameters related to the magnetic field can be found in each test condition used.

Figure 3. Gray magnet 0.55T.

Table 3. Test conditions. B denotes the intensity of the magnetic field in Gauss, t denotes the time the fluid was exposed to the magnetic field and Ha denotes the Hartmann number.

Flow rate (l/h)	300	600
Mean velocity (m/s)	0.88	1.75
Reynolds number (Re)	9650	19300
B.v (G.m/s)	4823	9646
B.v.t (G.m) total	3080	3080
B.v.t (G.m) effective	2200	2200
Ha	0,17	0,17
Ha/Re	2.10^{-5}	9.10^{-6}

Table 4 presents the supersaturation and the saturation index for the calcite after the reaction of calcium chloride with sodium bicarbonate, as well as the specific mass and dynamic viscosity of the solution formed.

Table 4. Calcite parameters in solution.

S	SI	$\rho(kg/m^3)$	$\mu(Pa.s)$
255	3.4	1000.46	0.001

The scaling tests monitor the differential pressure across the sliding sleeve valve. As the scaling occurs, the pressure drop across the valve increases. As this process evolve, there is point in time where the differential pressure increases exponentially. For security reasons, every test is finished when the pressure drop reaches a value of 2.5 bars.

At the end of each test, the material deposited in small sections of tube are dried in a desiccator for about 4 hours and then weighed. Such weighing sections were made of steel, 11 cm long and with an internal diameter of 11 mm.

The suspended particles are characterized in terms of particle size using the Mastersizer equipment and the number of particles using the Pamas equipment. The deposited fouling material was characterized by scanning electron microscopy (MEV) and X-ray diffraction (DRX).

4. RESULTS

The results and discussions will be presented below and according to the different experimental positions tested for the valve as well as for the magnet and in different Reynolds numbers.

4.1 Influence of the valve position

Figure 4 presents the differential pressure for the total time of the experiment for different valve positions in relation to the injection in the condition of 300 L/h of flow.

The deposition of the scaling material results in a reduction of the effective diameter, which leads to an increase in the local differential pressure in the tube section along the time of the experiment. Figure 4 shows that the experiments with the valve located at greater distances from the injection took longer to increase the differential pressure. This behaviour is due to the decrease in the saturation index along the pipe. Indeed, the chemical reaction is occurring since the pipe inlet and scales are being formed, most strongly in the entrance region of the pipe.

4.2 Influence of the magnetic field on different valve positions

Figures 5, 6, 7, 8 and 9 show the differential pressure over the total experiment time for different positions of the magnetic device at different valve positions. The presented curves correspond to the average of the replicates of the experiments carried out and the horizontal bars correspond to the uncertainty related to the experiment time.

Figures 5, 6, 8 and 9 show that the results with the valve positioned at 0.7 m, 3 m, 41 m and 45.6 m from the injection did not show a significant gain in time for the different positions and configurations of the magnetic field. Thus, both for the valve positioned at the beginning of the straight section and for the prototype positioned at the end of the straight section of pipe, there was no significant influence of the magnetic device. However, when analyzing Figure 7, it is possible to observe a more significant delay in the experiment time for the magnetic field positioned downstream of the solutions and upstream of the valve in the attractive configuration of the magnets.

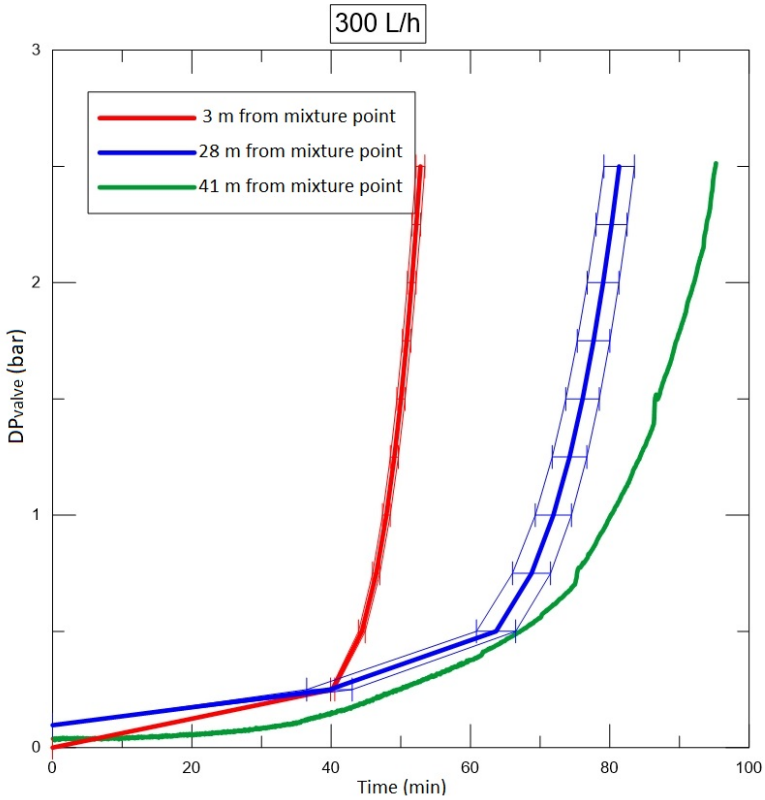

Figure 4. Time evolution of the differential pressure for different valve positions.

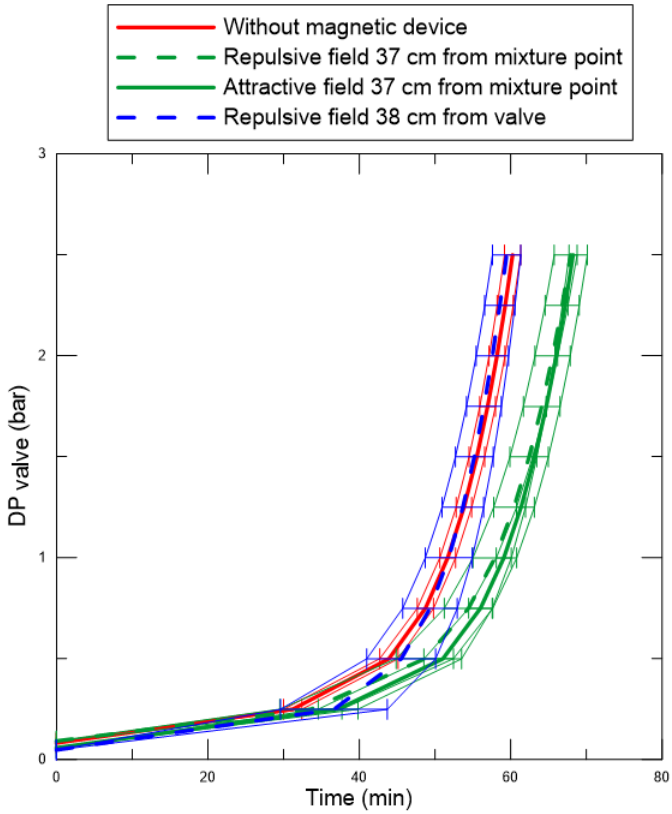

Figure 5. Time evolution of the differential pressure for the valve located at 0.7 m from the injection.

4.3 Reynolds' Influence

Valve at 28 m: Figures 10 and 11 show the result of the pressure drop in the valve over time in different magnet positions for two different Reynolds values.

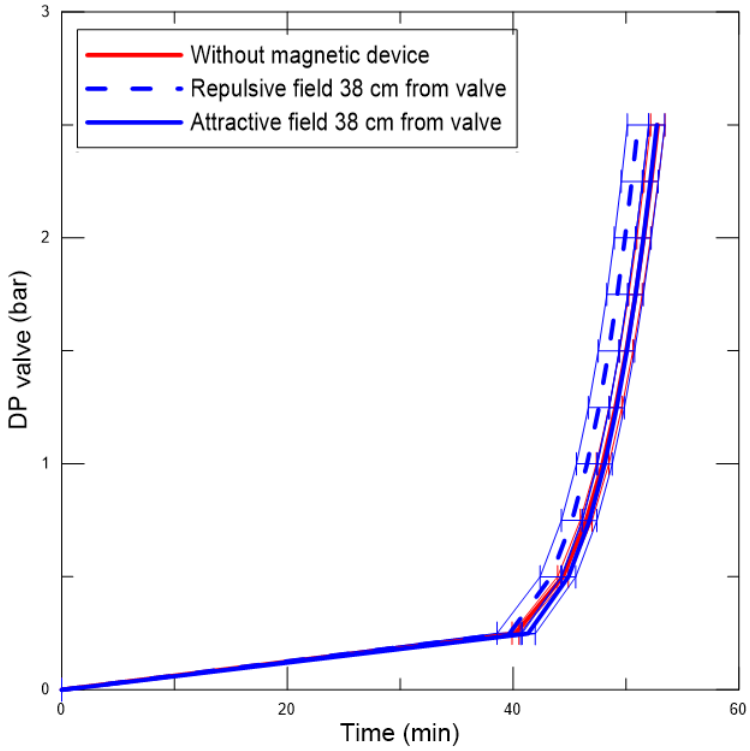

Figure 6. Time evolution of the differential pressure for the valve located at 3 m from the injection.

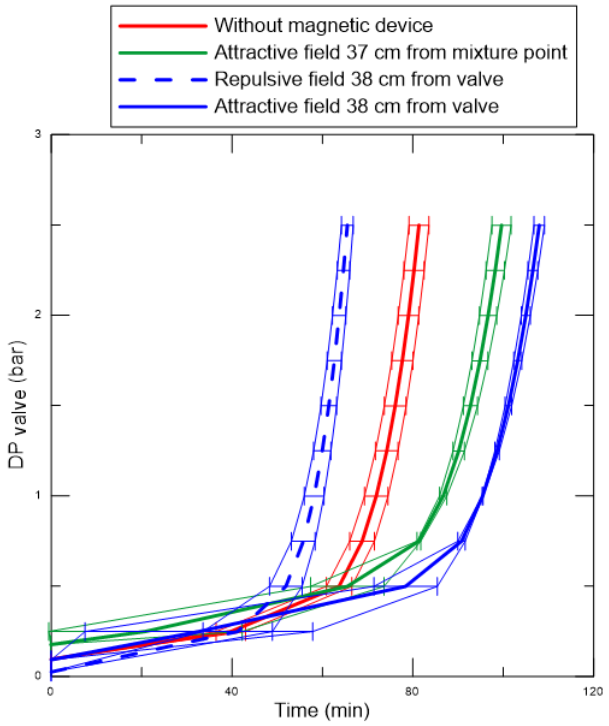

Figure 7. Time evolution of the differential pressure for the valve located at 28 m from the injection.

The results, for different Reynolds values, of the deposition rate along the different distances of the flow loop can be found in Figures 12 and 13.

Figures 10 and 11 show that the results of experiments carried out at higher Reynolds numbers (600 l/h) did not show a significant delay compared with those observed for the lower Reynolds numbers (300 l/h).

With regard to the deposition rate, Figures 12 and 13 show that for both analyzed situations, without device and with an attractive field upstream of the valve, the standardized deposition rate was lower for the higher Reynolds values.

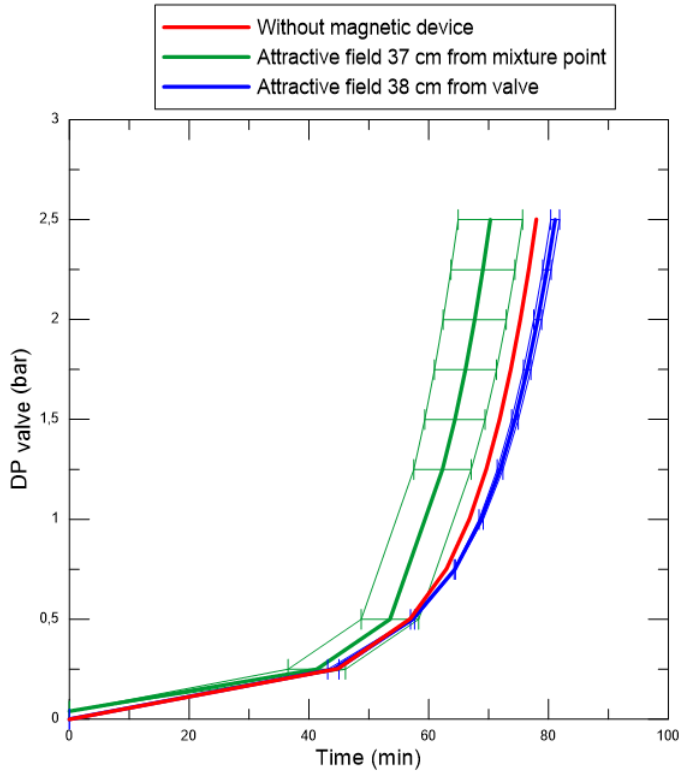

Figure 8. Time evolution of the differential pressure for the valve located at 41 m from the injection.

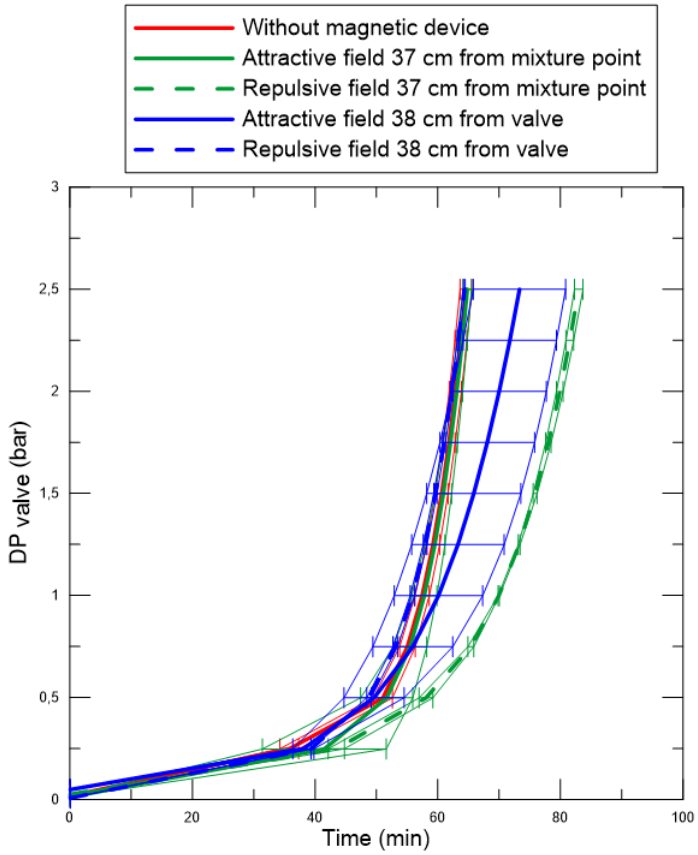

Figure 9. Time evolution of the differential pressure for the valve located at 45.6 m from the injection.

5. CONCLUSION

The magnetic field has the effect of delaying the time for blocking the sliding sleeve valve, when positioned close to the valve. The configuration that provided the best results on terms on mitigation was the valve positioned 28 m from the

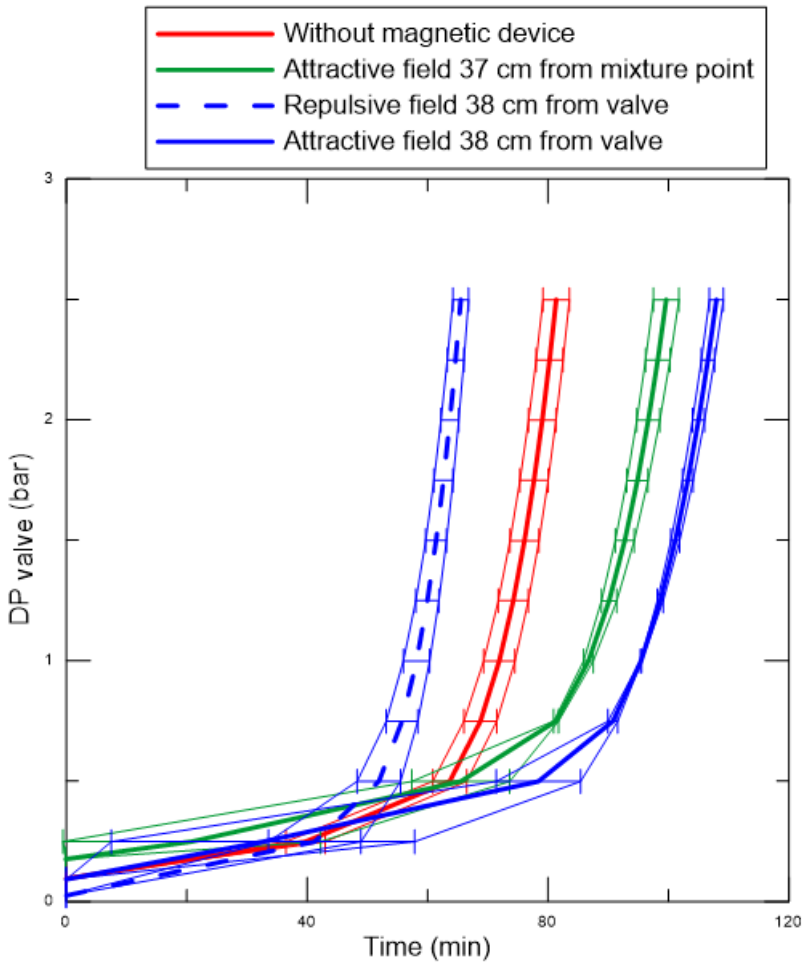

Figure 10. Time evolution of the differential pressure for the valve located at 28m with a flow rate of 300 L/h.

injection with the magnet positioned upstream of the valve, for the lower Reynolds number. The effect of the magnetic field was more pronounced for the lowest Reynolds numbers in general. Higher values of standardized deposition rates were observed for lower Reynolds numbers. The different locations of the valve along the flow loop means that, for each condition, the valve is subjected to different saturation indexes, where the scaling phenomena is evolving in different stages. Indeed, in the beginning of the pipe, nucleation is dominating, while further downstream crystal growth and agglomeration might be predominant. The scale grow in the pipe wall is then ruled by ionic deposition in the inlet region and from the around 25m downstream particle deposition becomes predominant. These chemical and kinetic processes are intrinsically related to the flow dynamics. As the Reynolds number increases, more calcium ions are being directed to the surface, though the mean time for the crystal growth and agglomeration inside the pipe decreases. Further investigation is needed so that we can relate the observed experimental results shown in this work with the characteristics of the solutions, the kinetics and flow dynamics of the problem.

6. ACKNOWLEDGEMENTS

We thank PETROBRAS for providing the valve and the financial support.

7. REFERENCES

Auerbach, M.H., Reimer, R.A., Olander, R.G. and Rapier, P.M., 1983. "A Calcium Carbonate Scale Inhibitor for Direct-Contact Binary Geothermal Service". *Journal of Petroleum Technology*, Vol. 35, No. 08, pp. 1546–1552. ISSN 0149-2136. doi:10.2118/10607-PA. URL `http://www.onepetro.org/doi/10.2118/10607-PA`.

Cowan, J.C. and Weintritt, D.J., 1976. *Water-formed scale deposits*. Gulf Publishing Company, Book Division.

Frenier, W.W. and Ziauddin, M., 2008. *Formation, removal, and inhibition of inorganic scale in the oilfield environment*. Society of Petroleum Engineers Richardson, TX.

Haghighi, H., 2009. *Phase equilibria modelling of petroleum reservoir fluids containing water, Hydrate Inhibitors and Electrolyte Solutions*. Ph.D. thesis, Heriot-Watt University Institute.

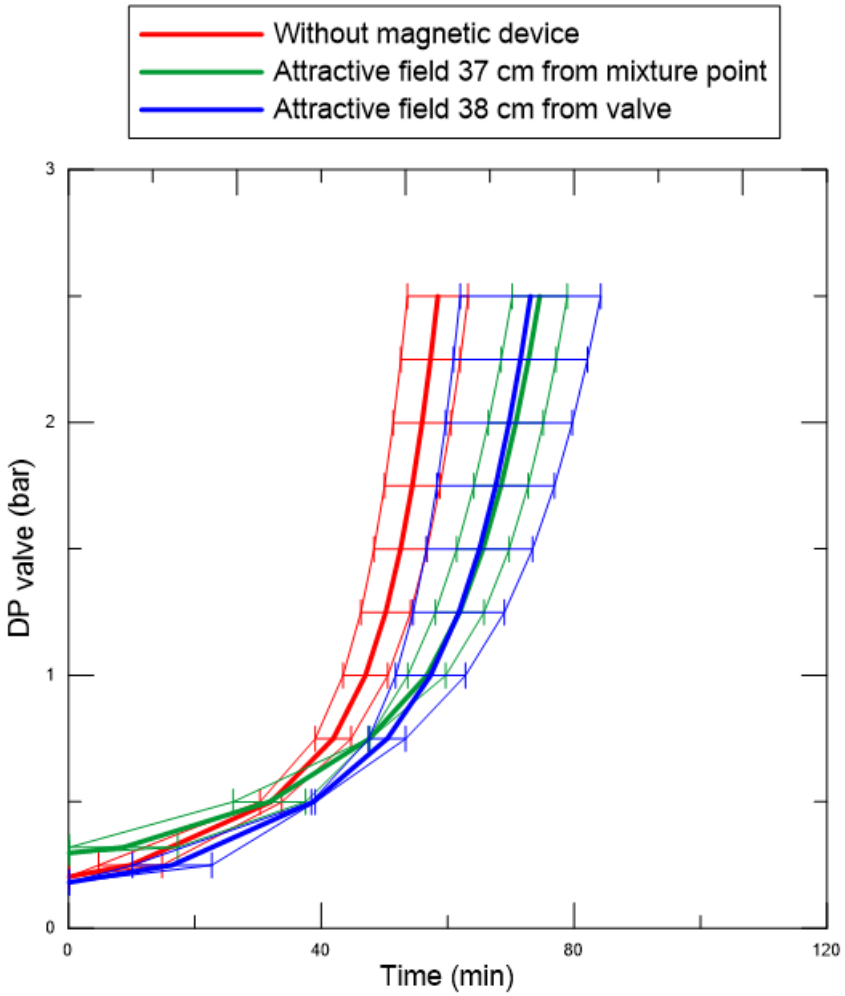

Figure 11. Time evolution of the differential pressure for the valve located at 28m with a flow rate of 600 L/h.

Kokal, S.L. and Sayegh, S.G., 1995. "Asphaltenes: The Cholesterol Of Petroleum". In *Middle East Oil Show*. Society of Petroleum Engineers, Vol. 14, pp. 646–657. doi:10.2118/29787-MS. URL http://www.onepetro.org/doi/10.2118/29787-MS.

Liu, Z. and Dreybrod, W., 1997. "Dissolution kinetics of calcium carbonate minerals in H2O-CO2 solutions in turbulent flow: The role of the diffusion boundary layer and the slow reaction H2O + CO2 → H+ + HCO3-". *Geochimica et Cosmochimica Acta*, Vol. 61, No. 14, pp. 2879–2889. ISSN 00167037. doi:10.1016/S0016-7037(97)00143-9. URL https://linkinghub.elsevier.com/retrieve/pii/S0016703797001439.

Mackay, E., Jordan, M. and Torabi, F., 2003. "Predicting Brine Mixing Deep Within the Reservoir and Its Impact on Scale Control in Marginal and Deepwater Developments". *SPE Production & Facilities*, Vol. 18, No. 03, pp. 210–220. ISSN 1064-668X. doi:10.2118/85104-PA. URL http://www.onepetro.org/doi/10.2118/85104-PA.

Merdhah, A.B., 2007. "The study of scale formation in oil reservoir during water injection at high-barium and high-salinity formation water". *Marine Science & Tchnology seminar*, pp. 1–189.

Nasr-El-Din, H.A. and Al-Humaidan, A.Y., 2001. "Iron Sulfide Scale: Formation, Removal and Prevention". In *Proceedings of International Symposium on Oilfield Scale*. Society of Petroleum Engineers. ISBN 9781555639150. doi:10.2523/68315-MS. URL http://www.spe.org/elibrary/servlet/spepreview?id=00068315.

Nichols, D.A., Frigo, D.M. and Graham, G.M., 2016. "Advances in Understanding Effects of Shear and Turbulence on Scale Formation, Adhesion and Growth on Surfaces". In *SPE International Oilfield Scale Conference and Exhibition*. Society of Petroleum Engineers. ISBN 9781613994559. doi:10.2118/179903-MS. URL http://www.onepetro.org/doi/10.2118/179903-MS.

Nikpoor, M.H., Dejam, M., Chen, Z. and Clarke, M., 2016. "Chemical–Gravity–Thermal Diffusion Equilibrium in Two-Phase Non-isothermal Petroleum Reservoirs". *Energy & Fuels*, Vol. 30, No. 3, pp. 2021–2034. ISSN 0887-0624. doi:10.1021/acs.energyfuels.5b02753. URL https://pubs.acs.org/doi/10.1021/acs.energyfuels.5b02753.

Obidi, O., Muggeridge, A.H. and Vesovic, V., 2017. "Analytical solution for compositional profile driven by gravitational segregation and diffusion". *Physical Review E*, Vol. 95, No. 2, p. 022138. ISSN 2470-0045. doi:

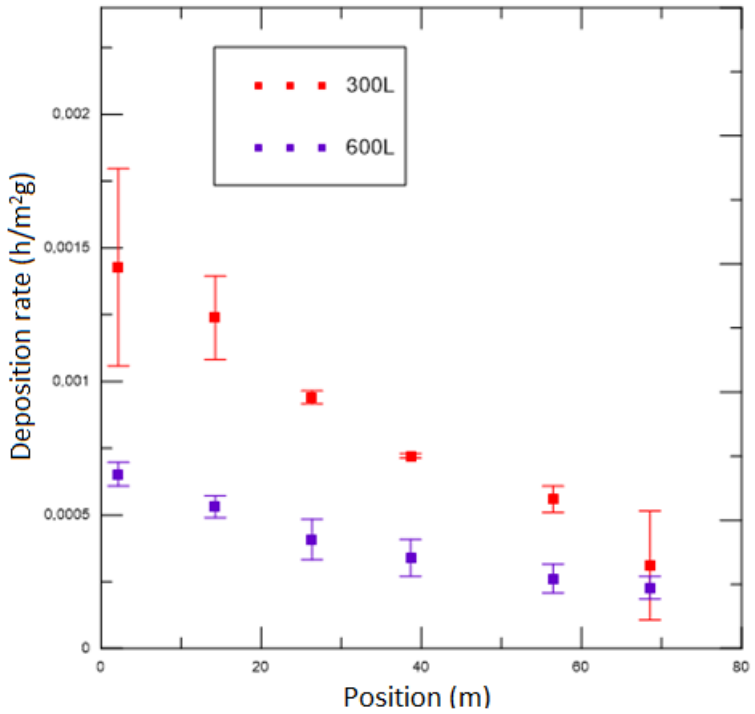

Figure 12. Deposition rate for the valve located at 28m and with a flow rate of 300 L/h.

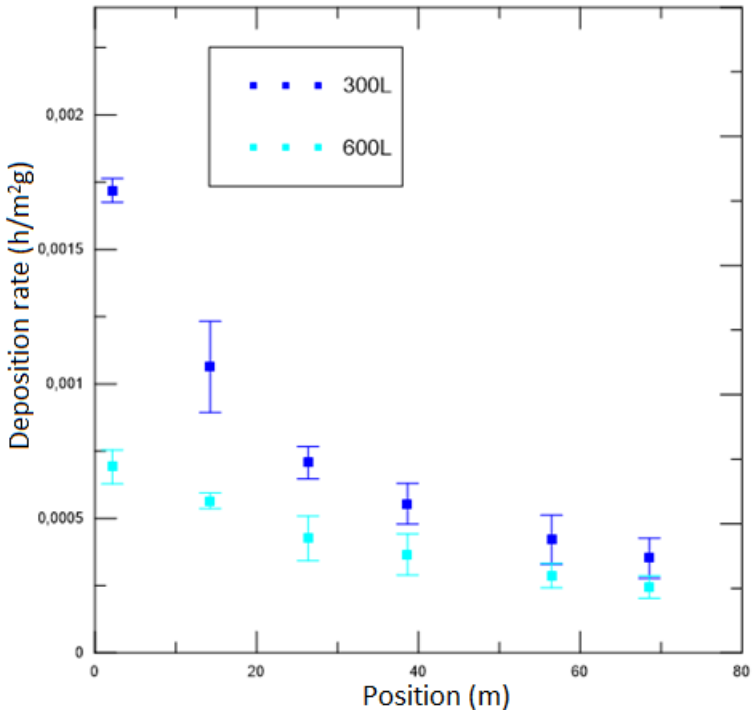

Figure 13. Deposition rate for the valve located at 28m and with a flow rate of 600 L/h.

10.1103/PhysRevE.95.022138. URL https://link.aps.org/doi/10.1103/PhysRevE.95.022138.

Oddo, J. and Tomson, M., 1989. "A Discussion of Calcium Carbonate Scaling Problems and Solutions With Respect to Produced Brines". In *SPE Annual Technical Conference and Exhibition*. Society of Petroleum Engineers. doi: 10.2118/19763-MS. URL http://www.onepetro.org/doi/10.2118/19763-MS.

Rousseau, G., Zhou, H. and Hurtevent, C., 2001. "Calcium Carbonate and Naphthenate Mixed Scale in Deep-Offshore Fields". In *Proceedings of International Symposium on Oilfield Scale*. Society of Petroleum Engineers. ISBN 9781555639150. doi:10.2523/68307-MS. URL

http://www.spe.org/elibrary/servlet/spepreview?id=00068307.

Shepherd, A.G., 2008. *A Mechanistic Analysis of Naphthenate and Carboxylate Soap-Forming Systems in Oilfield Exploration and Production Submitted for the degree of Doctor of Philosophy School of Engineering and Physical Sciences December 2008*. Ph.D. thesis, Heriot-Watt University. URL https://pdfs.semanticscholar.org/6e35/ad0ddbc5d125344d3191aa3b8a9ffdc9fcf8.pdf.

Szikszay, M., 1993. "Geoquímica das águas". *Boletim IG-USP. Série Didática*, Vol. 7, No. 5, p. 1. ISSN 2316-896X. doi:10.11606/issn.2316-896X.v0i5p1-166. URL http://www.revistas.usp.br/bigsd/article/view/45351.

Taheri, A., Masoudi, R., Zahedzadeh, M., Ataei, A. and Fakhri, H., 2008. "Simulation and Experimental Studies of Mineral Scale Formation Effects on Performance of an Iranian Carbonate Oil Reservoir under Water Injection". In *SPE International Oilfield Scale Conference*. Society of Petroleum Engineers, pp. 1–13. ISBN 9781605603414. doi:10.2118/113109-MS. URL http://www.onepetro.org/doi/10.2118/113109-MS.

Yan, F., Zhang, F., Bhandari, N., Ruan, G., Alsaiari, H., Dai, Z., Liu, Y., Zhang, Z., Lu, Y.T., Deng, G., Kan, A. and Tomson, M., 2017a. "The Effect of Turbulence on Mineral Scale Control in Oilfield". In *SPE International Conference on Oilfield Chemistry*. Society of Petroleum Engineers, Vol. 2017-April, pp. 869–883. ISBN 9781510842045. ISSN 10461779. doi:10.2118/184524-MS. URL http://www.onepetro.org/doi/10.2118/184524-MS.

Yan, F., Zhang, F., Bhandari, N., Ruan, G., Alsaiari, H., Dai, Z., Liu, Y., Zhang, Z., Lu, Y.T., Deng, G., Kan, A. and Tomson, M., 2017b. "The effect of turbulence on mineral scale control in oilfield". *Proceedings - SPE International Symposium on Oilfield Chemistry*, Vol. 2017-April, pp. 170–180. ISSN 10461779. doi:10.2118/184524-ms.

8. RESPONSIBILITY NOTICE

The authors are solely responsible for the printed material included in this paper.